Spin-orbit splitting in the HgTe surface quantum well

2001 J. Phys.: Condens. Matter 13 851

(http://iopscience.iop.org/0953-8984/13/5/306)

INSTITUTE OF PHYSICS PUBLISHING JOURNAL OF PHYSICS: CONDENSED MATTER

J. Phys.: Condens. Matter **13** (2001) 851–858 www.iop.org/Journals/cm PII: S0953-8984(01)16286-7

Spin–orbit splitting in the HgTe surface quantum well

V F Radantsev[1], A M Yafyasov[2], V B Bogevolnov[2] and I M Ivankiv[2]

[1] Institute of Physics and Applied Mathematics, Ural State University, Ekaterinburg 620083, Russia
[2] Institute of Physics, St Petersburg State University, St Petersburg 198904, Russia

E-mail: victor.radantsev@usu.ru

Received 11 August 2000, in final form 8 January 2001

Abstract

Two-dimensional electron gas at the anodic oxide–HgTe(110) interface is studied experimentally (by the magnetocapacitance spectroscopy method) and theoretically for carrier surface density up to 6×10^{12} cm^{-2}. The measurements show the population of up to four subbands with well-resolved Rashba spin splitting in the Fourier transforms. The carrier distribution among the electric subbands agrees with the theory. However, the experimental relative differences of occupancies of spin sub-subbands (0.17–0.3) exceed the calculated ones (0.14). This discrepancy indicates an interface contribution to the spin–orbit splitting. The partial capacitance oscillations for different spin branches in the ground subband differ not only in period but also in amplitude. Because of this, the measured effective cyclotron masses in this subband correspond to the theoretical values for the high-energy spin branch whereas in the excited subbands each corresponds to an average over two branches.

1. Introduction

The energy spectra of low-dimensional systems based on the classical gapless semiconductor HgTe have been investigated mainly for the superlattices CdTe–HgTe [1]. The most interesting features of an electron spectrum caused by the specificity of a 'gapless state' can be expected in asymmetrical quantum wells. Because of the small effective mass and strong spin–orbit interaction, the spin splitting of a spectrum by an asymmetrical electric field in zero magnetic field (the Rashba effect) in narrow-gap (and especially in gapless) semiconductors far exceeds those for wide-gap materials. This advantage makes these semiconductors preferred for application in spintronic devices (spin-polarized field-effect transistors).

Only recently have modulation-doped HgTe/$Hg_{1-x}Cd_xTe$ single quantum wells been grown by molecular beam epitaxy and magnetotransport studies performed. In the work [2], it was found that the spin splitting in an asymmetrically doped well is larger than that in a symmetrical one, and it increases with decreasing magnetic field. But no beat patterns have been observed in SdH oscillations, which are a characteristic feature of the Rashba effect. The most asymmetrical quantum wells are implemented in metal–insulator–semiconductor (MIS)

0953-8984/01/050851+08$30.00

structures. Another advantage of this system is the opportunity it affords to vary the depth of a quantum well over a wide range by applying a gate voltage. Thus we can change the number of 2D subbands, and their occupations, subband effective masses and spin–orbit splitting. This allows the extraction of extensive experimental information. Therefore, a more reliable test of the theoretical models can be made.

2. Samples and experimental methods

The MIS structures that we studied in this work were fabricated from HgTe(110) single crystals with a ∼100 nm thick anodic oxide film, grown in a solution of 0.1 M KOH in 90% ethylene glycol/10% H_2O at 0.5 mA cm^{-2}. The acceptor concentration ($N_A - N_D = 0.9 \times 10^{16}$ cm^{-3}) and the Fermi energy in the bulk (1.9 meV) were determined by Hall-effect measurements performed at variable temperatures and magnetic field strengths. The traditional magnetotransport methods cannot be used for the study of either the accumulation or the inversion channels of semimetals. The differential capacitance C (and derivative $\mathrm{d}C/\mathrm{d}V_g$ with respect to the gate voltage V_g) of the capacitors in quantizing magnetic fields $B = 0$–6 T were measured in the dark (typically at 1 MHz and for a test signal amplitude of 5 mV) to investigate the parameters of the 2D electron gas (the subband occupations, effective masses, parameters of spin–orbit splitting and parameters of broadening of the Landau levels) in the inversion layer. For correct analysis of the oscillation amplitudes (used for determination of the effective masses and Landau-level broadening parameters), the $C(V_g)$ and $C(B)$ plots were transformed into the dependencies $C_{sc}(V_g)$ and $C_{sc}(B)$ ($C_{sc} = C_{ox}C/A(C_{ox} + C)$ is the specific capacitance of the space-charge region, C_{ox} is the oxide capacitance and A is the gate area). The oxide capacitance C_{ox} was determined from the capacitance of the MOS structures in a strong-accumulation regime.

The capacitance magneto-oscillations due to the Landau quantization of the subband spectrum were observed in both the $C(V_g)$ and $C(B)$ dependencies (figures 1 and 2). The measurements show the population up to four two-dimensional subbands. The individual spin components have not been observed in the magneto-oscillations even for the lowest Landau levels. However, the beats of the oscillations and the well-resolved split of the Fourier spectra into two lines point to Rashba splitting in each 2D subband at subband concentrations that are not too high (see below):

$$n_i = n_i^+ + n_i^-$$

($n_i^\pm$ are the populations in the high- and low-energy spin branches of the ith 2D subband). The oscillations for the ground subband were observed only at gate voltages which are larger than the value V_m corresponding to the minimum of the $C(V_g)$ characteristic (the capacitance–voltage characteristics are those of typical low-frequency behaviour because of the absence of a gap). At the same time, the cut-off voltage V_{st} of the $n_0(V_g)$ dependence was 0.3–0.4 V less than V_m. Thus, because of the strong quenching of oscillations on the falling branch of the $C(V_g)$ curve, we cannot study the parameters of the $i = 0$ subband at

$$n_0 < n_0(V_m) \approx (1\text{–}2) \times 10^{11} \text{ cm}^{-2}.$$

Using Fourier filtration and inverse Fourier transformation, we extracted from the experimental $C_{sc}(B)$ traces the partial capacitance magneto-oscillations associated with different spin branches (figure 2). It should be noted that the partial oscillations for different spin sub-subbands differ not only in period (which leads to the oscillation beats) but also in amplitude, especially for the ground subband.

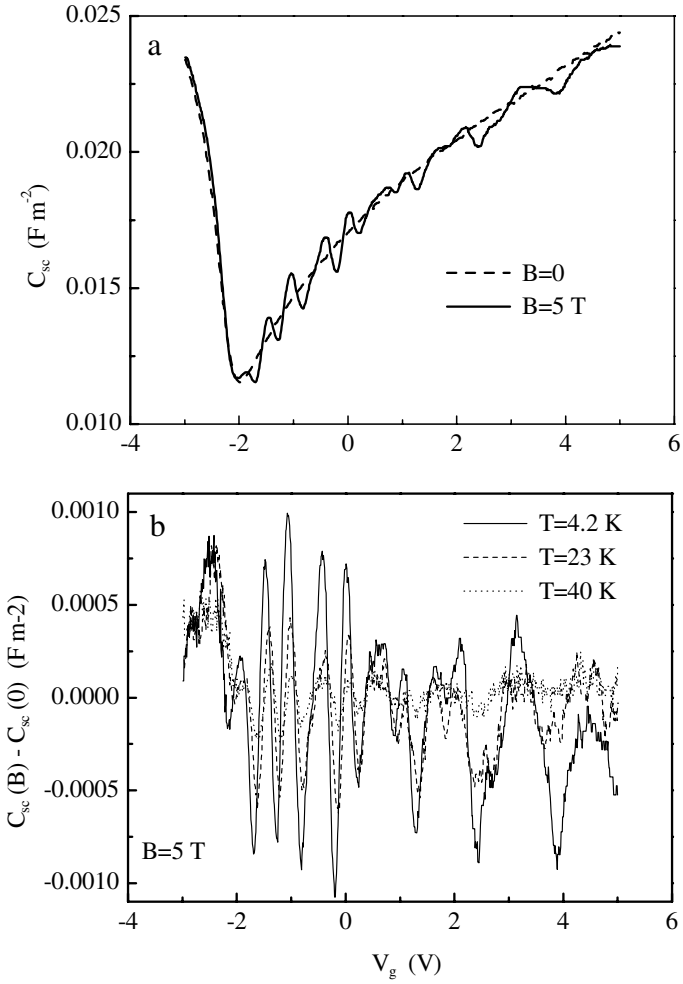

Figure 1. Space-charge-region capacitance–gate voltage characteristics (a) and the magneto-capacitance oscillations $C_{sc}(B) - C_{sc}(0)$ (b) as functions of V_g for the HgTe MOS structure.

3. Results and discussion

The distribution of carriers among the spin-split 2D subbands given by the Fourier transforms and the subband cyclotron effective masses determined from the temperature dependencies of the amplitudes of the original $C_{sc}(B)$ oscillations are plotted in figure 3 versus the total 2D concentration $n_s = \sum n_i$. The values of n_s agree well with the densities of charge induced in the space-charge region

$$eN_s = C_{ox}(V_g - V_{st} - V_s)/A$$

(V_s is the band bending). In this figure we also give the theoretical dependencies calculated in the 6×6 $\boldsymbol{k} \cdot \boldsymbol{p}$ Kane model as in the work [3]. The change of charge in the depletion layer with V_s in the inversion band-bending range (in gapless semiconductors such changes can be quite significant) is taken into account in the calculation. The temperature dependencies of the band parameters and bulk Fermi energy are accounted for in the calculations. The

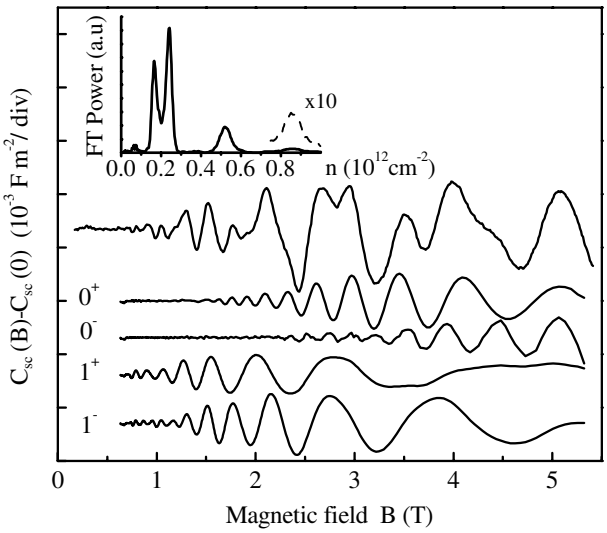

Figure 2. Partial magnetocapacitance oscillations for different spin branches $i^{\pm}$ extracted from the Fourier transform (FT) (shown in the inset) of the experimental $C_{sc}(B)$ trace (upper curve).

calculated dependencies $n_i(n_s)$ agree satisfactorily with the experimental ones; however, a large difference between the calculated and measured effective masses is obtained. The discrepancy is manifested also (especially in the low-n_s range) in a 'spin polarization'

$$\Delta n_i/n_i = (n_i^- - n_i^+)/(n_i^- + n_i^+)$$

shown in figure 4(a).

It should be noted that the requirement $Eg \ll 2\Delta/3$ ($\Delta = E(\Gamma_8) - E(\Gamma_7)$), accepted in the work [3], is insufficiently well satisfied for HgTe. We have carried out a further development of the theory within the scenario of [3], generalized by allowance for the Γ_7 band. The results of such self-consistent calculations are also given in figures 3 and 4. These calculations are in better agreement with the experimental masses. At the same time, the allowance for the Γ_7 band leads to a diminution of the Rashba splitting. As a result, the discrepancy with respect to the experimental values of $\Delta n_i/n_i$ actually increases slightly.

At $n_i > 2 \times 10^{12}$ cm^{-2} only a single line in the Fourier spectra for the $i = 0$ subband is observed; however, the concentrations associated with this line are the occupancies of a high-energy branch n_i^+ of a spectrum and not the average subband concentrations (see figure 3(a)). This is because the ratio of intensities of the Fourier lines (of the oscillation amplitudes) for the high-energy branch and low-energy branch I_i^-/I_i^+ decreases rapidly with increasing n_i (figure 4(b)). For the same reason, throughout the n_s-range, the effective masses for the ground subband determined from the initial $C_{sc}(B)$ plots correspond to a high-energy branch which gives the dominant contribution to the amplitude of the total oscillations. The values of m_{c0}^+ determined from the temperature dependencies of the partial oscillations $C_{sc}^+(B)$ directly confirm this conclusion. At the same time, for excited subbands, for which the amplitudes of oscillations for different branches are close, the measured effective masses are rather close to the average values calculated. Unfortunately, the relative weakness of the Rashba splitting in excited subbands impedes the extracting of partial oscillations at high temperatures and the precise definition of the sub-subband cyclotron masses is hampered.

It is shown in [4] that a difference in amplitude between different spin components of the oscillations is to be expected for 2D systems with strong spin–orbit interaction even if the

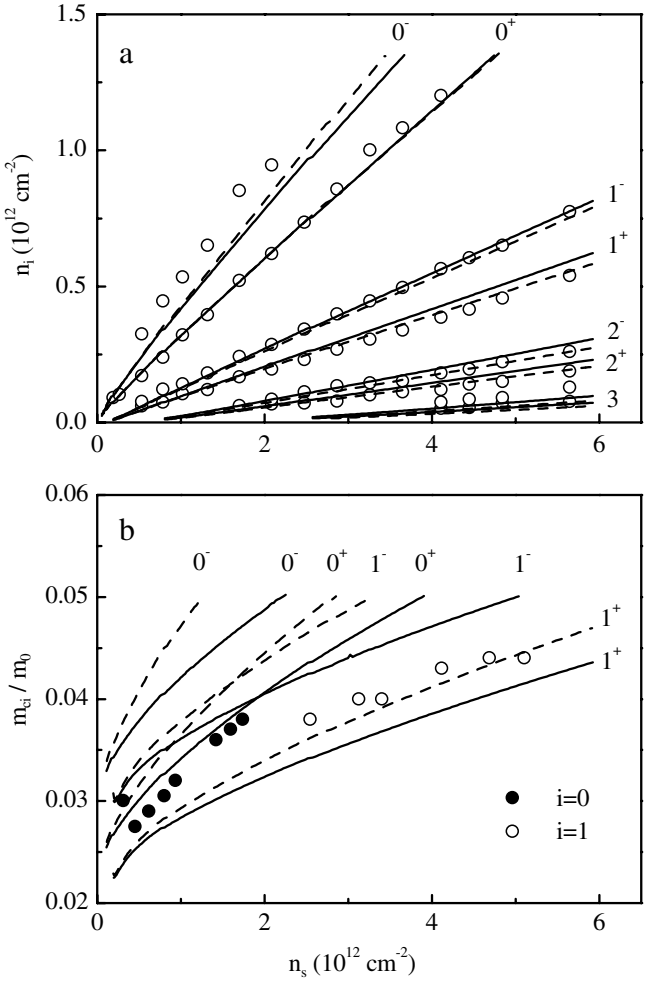

Figure 3. Calculated (curves) and measured (points) surface densities (a) and cyclotron masses (b) of 2D electrons in spin-split subbands. The theoretical dependencies are calculated with (——) and without (– – –) allowance for the Γ_7 band. The numbers on the curves are subband numbers.

relaxation times τ are equal. The reason is that although the density of states in branch $(-)$ is higher, the corresponding amplitudes may be less because of the larger cyclotron mass (low cyclotron energy). We performed a computer simulation of the oscillations, as was done in the work [4]. In the modelling, the surface potential and subband Fermi energies are supposed to be constant when the magnetic field is changing. An alternative model is based on the assumption that the surface density is fixed. However, the two models give indistinguishable results at large enough LL broadening (this is manifested by the cosine form of the experimental oscillations) [5].

The simulation shows that, in contrast to the case for the HgCdTe-based MIS structures, the big difference in amplitude of the partial oscillations for the $i = 0$ subband in the HgTe surface quantum wells investigated is caused only in part by the difference in cyclotron mass. The experimental $C(B)$ curves can be fitted by simulation only if we assume the relaxation time in a 0^- sub-subband to be less than that in a 0^+ branch. As an example, the Dingle

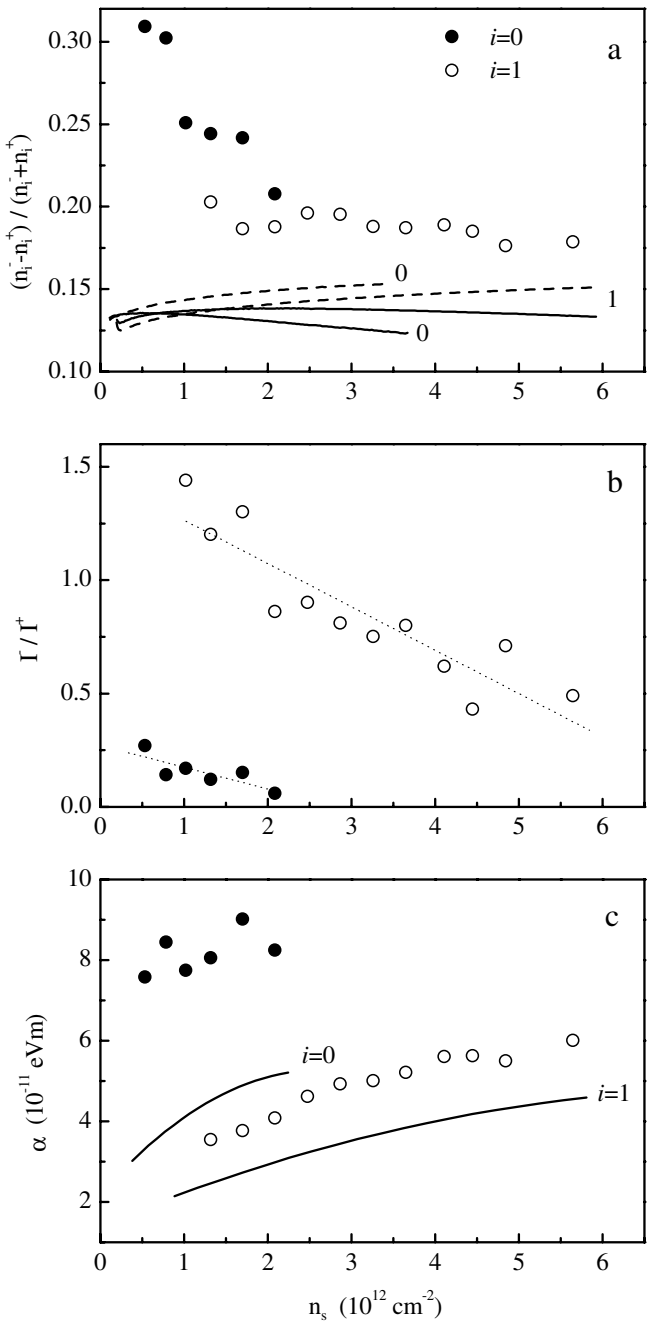

Figure 4. The relative difference of the occupancies of the spin-split sub-subbands (a), the ratio of the intensities of the Fourier lines for the low- and high-energy sub-subbands (b) and the Rashba parameter (c) versus n_s. The notation for the theoretical curves in panels (a) and (c) is the same as in figure 3. The lines in panel (b) are guides for the eye. However, it may be noted that the ratios I_i^-/I_i^+ determined from the Fourier spectra of the simulated oscillations are also close to these lines (the exact values of I_i^-/I_i^+ depend strongly and non-monotonically on the magnetic field ranges used in the Fourier transformation).

temperatures $T_D = \hbar/k_B 2\pi\tau$ corresponding to the oscillations in figure 2 are 14 K, 17 K, 9 K and 8 K for the 0^+, 0^-, 1^+ and 1^- branches, respectively. (At the same time, the Landau-level broadening parameters

$$\Gamma_i = \sqrt{2\hbar^2 eB/\pi\tau_i m_{ci}}$$

for the two spin branches are practically the same (3.8 meV $T^{-1/2}$ for $i = 0$)). The T_D-values estimated from the magnetic field dependencies of the amplitudes of the partial oscillations in the region of small magnetic field, from the fit of the absolute values of the capacitance oscillations and from the values of the magnetic field corresponding to the occurrence of oscillations are in good agreement. It should be emphasized that, in accordance with experiment, separate spin components are not exhibited in simulated $C(B)$ or $C(V_g)$ oscillations even for the lowest LLs for any reasonable broadening parameters and magnetic fields of experimental interest.

Let us now turn to the parameters of the spin–orbit splitting. It is conventional to characterize the zero-field splitting effect via the coefficient α (the Rashba parameter) in the term $\pm\alpha k$, linear in the wave vector, in the subband dispersion

$$\varepsilon_i^{\pm}(k) - \varepsilon_i(0) = \frac{\hbar^2 k^2}{2m_i} \pm \alpha k.$$

However, in the works [3, 6] it was shown that for Kane semiconductors not only the linear Rashba approach but also the Kane-like approximation [7]

$$\varepsilon_i^{\pm}(k) - \varepsilon_i(0) = \sqrt{(s\hbar k)^2 + m_i^2 s^4 \pm 2m_i s^2 \alpha_i k} - m_i s^2$$

(m_i is the bottom subband mass, $s = \sqrt{2/3}P/\hbar \approx 1.03 \times 10^8$ cm s^{-1} is the Kane velocity and P is the Kane momentum matrix element) are invalid for the description of spin-split subband dispersions. The splitting is not only saturated with increasing k, but also can reach a maximum and then decrease. Thus, strictly speaking, α is not a 'good' parameter in the general case (the value of α at the Fermi level is nearly twice that at small k, when the linear Rashba approximation holds [3]). However, we can consider α as an energy-dependent parameter and use its value at the Fermi level. Such a semiphenomenological approach is especially useful from the point of view of comparison of spin–orbit coupling constants for various quantum wells.

By taking the measured and calculated values of $\Delta n_i/n_i$ from the data in figure 4(a), we have estimated the parameter α (figure 4(c)) via the phenomenological formula

$$\alpha = \frac{\hbar^2\sqrt{\pi n_i}}{m_i}(1 - \sqrt{1 - (\Delta n_i/n_i)^2})^{1/2}$$

obtained for Kane-like subband dispersion in [7] (for a parabolic spectrum and at small α, this expression is reduced to a formula from [8]). The bottom subband masses m_i were determined from the fit of the Kane-like dispersion relationship to the dispersion numerically calculated without spin–orbit interaction. The values obtained, $\alpha \approx$ (2–8) $\times 10^{-11}$ eV m, are higher by an order of magnitude than those in the most extensively studied asymmetrical quantum wells based on InGaAs ($\alpha = (0.4\text{–}1.5) \times 10^{-11}$ eV m; see [8, 9] and references therein). This is not unexpected because of the smallness of the effective mass in HgTe. The increase in measured α with n_s (with increasing gate voltage V_g) exceeds the experimental error for the $i = 1$ subband and agrees with the theoretical prediction. This is in contrast to the case for the gated InGaAs structures, which manifest the opposite behaviour with increasing V_g [8, 9].

At the same time, both the $\Delta n_i/n_i(n_s)$ and the $\alpha(n_s)$ dependencies unambiguously show that the theory, which takes into account the contribution originating from the spatial charge

region alone, underestimates the zero-field splitting. Such a discrepancy is also inherent to InGaAs quantum wells, for which the experimental values of α exceed the calculated ones by a factor of 2–4 [8–10]. However, there are two contributions to the Rashba splitting: the pure field contribution induced inside the quantum well and the interface contribution, which is a result of the spin-dependent boundary conditions [6]. The latter adds to the total splitting [6, 8], contrary to what one would expect from Ando argumentation [11]. As the boundary contribution is expected to be fairly independent of the gate voltage, the fact that the difference between the experimental value of α and the calculated one (the field contribution) does not change with n_s supports the model considered. The difference is bigger for the ground subband, which lends further support, because the electrons in this subband are more strongly pushed toward the interface.

Some difficulty with this explanation lies in the fact that the potential barriers at the interfaces in MOS structures are vastly higher than those in semiconductor heterostructures. Thus, the amplitude of a wave function at an interface and hence the boundary contribution to α should be small. It is possible that there is a significant contribution from the transition region near the interface with the oxide. Quantitative estimation would require extensive knowledge about this region.

Acknowledgments

This work was supported by the project Esprit N 28890 NTCONGS EC (European Community), by Award No REC-005 of the US Civilian Research and Development Foundation (CRDF) and by a Grant from the Education Committee of Russia.

References

[1] Hoffman C A, Neyer J R, Bartoli F J, Lansari Y, Gook J W and Schetzima J F 1991 *Phys. Rev.* B **44** 8376
[2] Zhang X C, Pfeuffer-Jeschke A, Ortner K, Goschenhofer F, Becker C R, Landwehr G and Remenyi G 2000 *Proc. 9th Int. Conf. on Narrow Gap Semiconductors* (Berlin: Humboldt University Press) p 213
[3] Radantsev V F, Deryabina T I, Kulaev G I and Rumyantsev E L 1996 *Phys. Rev.* B **53** 15 756
[4] Radantsev V F 1999 *Zh. Eksp. Teor. Fiz.* **115** 1002 (Engl. Transl. 1999 *Sov. Phys.–JETP* **88** 552)
[5] Bassom N J and Nicholas R J 1992 *Semicond. Sci. Technol.* **7** 810
[6] De Andrada E A, Silva E, La Rocca G C and Bassani F 1997 *Phys. Rev.* B **55** 16 293
[7] Radantsev V F 1989 *Zh. Eksp. Teor. Fiz.* **96** 1793 (Engl. Transl. 1989 *Sov. Phys.–JETP* **69** 1012)
[8] Engels G, Lange J, Schapers Th and Luth H 1997 *Phys. Rev.* B **55** R1958
[9] Nitta J, Akazaki T, Takayanagi H and Enoki T 1997 *Phys. Rev. Lett.* **78** 1335
[10] Yamada S, Sato Y, Gozu S and Kikutani T 2000 *Proc. 9th Int. Conf. on Narrow Gap Semiconductors* (Berlin: Humboldt University Press) p 207
[11] Ando T, Fowler A B and Stern F 1982 *Rev. Mod. Phys.* **54** 494